Journal of Solid State Chemistry **158,** 87–93 (2001)
doi:10.1006/jssc.2001.9100, available online at http://www.idealibrary.com IDEAL®

Hydrothermal Syntheses, Structures, and Magnetic Properties of the U(IV) Fluorides $(C_5H_{14}N_2)_2U_2F_{12}\cdot 5H_2O$ and $(NH_4)_7U_6F_{31}$

Philip M. Almond,* Laura Deakin,† Arthur Mar,† and Thomas E. Albrecht-Schmitt*,[1]

*Department of Chemistry, Auburn University, Auburn, Alabama 36849; and †Department of Chemistry, University of Alberta, Edmonton, Alberta T6G 2G2, Canada

Received September 19, 2000; in revised form December 19, 2000; accepted January 19, 2001

The U(IV) fluorides $(C_5H_{14}N_2)_2U_2F_{12}\cdot 5H_2O$ (AU1-2) and $(NH_4)_7U_6F_{31}$ have been prepared from the reaction of UO_3 with HF and homopiperazine ($C_5H_{12}N_2$) at 180°C in aqueous media. AU1-2 contains dodecahedral UF_8 units that share two edges to form $^1_\infty[UF_4F_{4/2}]$ one-dimensional chains. The fluoride ligands form hydrogen bonds with the diprotonated homopiperazinium cations to yield channels running down the *a* axis that contain occluded water molecules. $(NH_4)_7U_6F_{31}$ is isostructural with $Na_7Zr_6F_{31}$, forming a three-dimensional network consisting of edge- and corner-sharing UF_8 square antiprisms that create cubooctahedral clusters and small intersecting channels. A disordered fluoride anion resides in the cubooctahedral cavities and the ammonium cations partially fill the channels. AU1-2 and $(NH_4)_7U_6F_{31}$ display similar magnetic behavior with μ_{eff} (300 K) = 3.05 and 3.03 μ_B/U(IV) and $\theta = -97$ and -126 K, respectively. Crystallographic data: AU1-2, monoclinic, space group $P2_1/n$, $a = 6.545(3)$ Å, $b = 19.90(1)$ Å, $c = 19.07(1)$ Å, $\beta = 98.89(4)°$, $Z = 4$, $\lambda = 0.71073$ Å, $R(F) = 0.0395$ for 293 parameters with 3282 reflections with $I > 2\sigma(I)$; $(NH_4)_7U_6F_{31}$, rhombohedral, space group $R\bar{3}$, $a = 15.371(3)$ Å, $c = 10.791(3)$ Å, $Z = 3$, $\lambda = 0.71073$ Å, $R(F) = 0.0242$ for 82 parameters with 841 reflections with $I > 2\sigma(I)$

Key Words: **hydrothermal synthesis; uranium fluorides; one-dimensional structures.**

INTRODUCTION

Hydrothermal reactions of uranium oxides and uranyl acetate with a wide variety of mineralizing agents in the presence of structure-directing amines have afforded a large series of low-dimensional and open-framework fluorides (1–7), oxyfluorides (5, 6, 8–10), phosphates (11), and molybdates (12). While some of these organically templated uranium-containing compounds possess known structures for the inorganic framework, as found in $(H_3N(CH_2)_nNH_3)U_2F_{10}$ ($n = 2$, 3, 5, 6) (1, 2, 6), the use of milder conditions (< 250°C) has led to new structure types such as those found in $(C_6H_{14}N_2)_2(U_3O_4F_{12})$ (10) and $(C_5H_{14}N_2)(U_2F_{10}(H_2O))$ (7). This structural diversity is derived in part from the flexibility of coordination environments possible around uranium, in the form of pentagonal bipyramids, dodecahedra, square antiprisms, and bicapped and tricapped trigonal prisms.

The isolation of organically templated uranium fluorides and oxyfluorides has revived interest in the magnetic properties of actinide-containing compounds. In two-dimensional $(C_2H_{10}N_2)U_2F_{10}$ (**AU2-1**), weak ferromagnetic interactions have been observed, while one-dimensional $(C_5H_{14}N_2)_2U_2F_{12}\cdot 2H_2O$ (**AU1-1**) displays a metamagnetic-like transition (6). While the magnetic behavior of U(IV) compounds has generally been interpreted on the basis of a $5f^2$ configuration with a $^3H_4$ ground state (13), there has been a lack of detailed magnetic analysis of low-dimensional uranium-containing compounds owing to complications arising from spin-orbit, crystal-field, and zero-field splitting effects on the temperature dependence of the susceptibility (14). Previous studies on monomeric octacoordinated U(IV) complexes have revealed effective moments ranging from 2.92 to 3.5 μ_B with Weiss constants ranging from $\theta = -50$ to -200 K (15). The effective moments for UCl_4 and UF_4 are 3.29 and 3.28 μ_B, respectively (16). Significant variation in U–U distances, which affects the magnetic behavior of these compounds, is often observed. However, long-range magnetic ordering has not yet been found for one-, two-, or three-dimensional U(IV) fluorides. Herein we report the hydrothermal syntheses, structural characterization, and magnetic properties of two U(IV) compounds containing UF_8 units, one-dimensional $(C_5H_{14}N_2)_2U_2F_{12}\cdot 5H_2O$ (**AU1-2**) and three-dimensional $(NH_4)_7U_6F_{31}$. The latter compound has been known since at least 1963 from X-ray powder diffraction data (17, 18), but no further structural characterization has ensued.

EXPERIMENTAL

Syntheses. UO_3 (99.8%, Alfa-Aesar), HF (48 wt%, Aldrich), and homopiperazine (98%, Aldrich) were used as

[1]To whom correspondence should be addressed. Fax: (334) 844-6959. E-mail: albreth@auburn.edu.

0022-4596/01 $35.00

received. Distilled and millipore-filtered water was used in all reactions. The resistance of the water was 18.2 MOhm. *While the UO_3 contains depleted U, standard precautions for handling radioactive materials should be followed.* Elemental (CHN) microanalyses were performed by Atlantic Microlab, Inc. All reactions were run in Parr 4749 23-ml autoclaves with PTFE liners. The naming system for these compounds stands for Auburn University, the dimensionality of the structure, and the compound number.

$(C_5H_{14}N_2)_2U_2F_{12}\cdot 5H_2O$(**AU1-2**). UO_3 (0.572 g, 2 mmol) and homopiperazine (301 mg, 3 mmol) were loaded in a 23-ml PTFE-lined autoclave. Water (1 ml) was then added to the solids followed by the dropwise addition of HF (0.54 ml, 15 mmol). The autoclave was sealed and placed in a box furnace that had been preheated to 180°C. After 72 h the furnace was cooled at 9°C/h to 23°C. The product consisted of a brown solution over a large bloom of elongated turquoise prisms (**AU1-2**), clusters of pale green cyrstals with a rectangular tabular habit (**AU2-3**) (7), dark green hexagonal tablets (**AU2-2**), and olive green truncated hexagonal bipyramids (**AU2-1**) (6). The mother liquor was decanted from the crystals, which were then washed with methanol and allowed to dry; yield (**AU1-2**), 722 mg (72% yield). Anal. calcd for $C_5H_{24}N_2F_{12}U_2$: C, 12.03; H, 3.84; N, 5.61. Found: C, 12.15; H, 3.66; N, 5.50.

$(NH_4)_7U_6F_{31}$. UO_3 (572 mg, 2 mmol) and homopiperazine (701 mg, 7 mmol) were loaded in a 23-ml PTFE-lined autoclave. Water (1 ml) was then added to the solids followed by the dropwise addition of HF (0.40 ml, 11 mmol). The autoclave was sealed and placed in a box furnace that had been preheated to 180°C. After 72 h the furnace was cooled at 9°C/h to 23°C. The product consisted of a viscous green solution over a few massive, nearly perfect, emerald green rhombohedral crystals. The mother liquor was decanted from the crystals, which were then washed with methanol and allowed to dry. Additional crystals of **AU1-2** grew from the mother liquor after several days. Yield of $(NH_4)_7U_6F_{31}$, 176 mg (25% yield) with one crystal making up 50 mg of the product mass. Anal. calcd for $H_{28}N_7F_{31}U_6$: H, 1.32; N, 4.57. Found: H, 1.31; N, 4.58.

Crystallographic studies. Intensity data were collected from single crystals of **AU1-2** and $(NH_4)_7U_6F_{31}$ with the use of a Nicolet R3M X-ray diffractometer. Data for each compound were processed and analytical absorption corrections were applied. The structures were solved by direct methods and refined using the SHELXTL-93 package (19). In the refinements for **AU1-2**, hydrogen atom positions for the homopiperazinium cations were calculated with isotropic riding temperature factors. Because the uranium atoms dominate the scattering, hydrogen positions for water molecules and ammonium cations could not be reliably determined in both structures and were not included in the structural models. The final refinement included displacement parameters for all nonhydrogen atoms and a secondary extinction parameter. The F(6) atom in $(NH_4)_7U_6F_{31}$ was disordered over six closely spaced positions near the center of a cubooctahedral cavity. As the composition of this phase is known to be variable (18), the occupancy of the F(6) site was refined, converging to 0.13(2). As refinement on occupancy for determining chemical composition is questionable at best (20, 21), the occupancy of this atom was set at 1/6, corresponding to the presence of exactly one F atom inside the cubooctahedral cavity. This results in the formulation of this compound as $(NH_4)_7U_6F_{31}$, which is consistent with chemical analyses. Some crystallographic details are listed in Table 1 for **AU1-2** and $(NH_4)_7U_6F_{31}$. The final positional parameters for **AU1-2** and $(NH_4)_7U_6F_{31}$ are given in Tables 2 and 3.

TABLE 1
Crystallographic Data for $(C_5H_{14}N_2)_2U_2F_{12}\cdot 5H_2O$ (AU1-2) and $(NH_4)_7U_6F_{31}$

Formula	$(C_5H_{14}N_2)_2U_2F_{12}\cdot 5H_2O$	$(NH_4)_7U_6F_{31}$
Formula mass (amu)	998.50	2143.47
Color and habit	Turquoise prism	Green rhombohedron
Crystal system	Monoclinic	Rhombohedral
Space group	$P2_1/n$ (No. 14)	$R\bar{3}$ (No. 148)
a (Å)	6.545(3)	15.371(3)
b (Å)	19.90(1)	15.371(3)
c (Å)	19.07(1)	10.791(3)
α (deg.)	90	90
β (deg.)	98.89(4)	90
γ (deg.)	90	120
V (Å^3)	2454(2)	2208.0(9)
Z	4	3
T (°C)	22	22
λ (Å)	0.710 73	0.710 73
Maximum 2θ (deg.)	50	50
Observed data $I>2\sigma(I)$	3282 ($R_{int}=0.0280$)	841 ($R_{int}=0.1122$)
ρ_{calcd} (g cm^{-3})	2.675	4.772
μ(Mo$K\alpha$) (cm^{-1})	133.00	330.89
$R(F)$ for $F_o^2>2\sigma(F_o^2)^a$	0.0395	0.0242
$R_w(F_o^2)^b$	0.0898	0.0557

$^aR(F)=\sum\|F_o|-|F_c\|/\sum|F_o|$.
$^bR_w(F_o^2)=[\sum[w(F_o^2-F_c^2)^2]/\sum wF_o^4]^{1/2}$.

Magnetic measurements. Magnetic data were measured on powders in gelcap sample holders with a Quantum Design PPMS 9 T magnetometer/susceptometer between 2 and 300 K and under applied fields up to 9 T. Magnetic susceptibility measurements were made under zero-field-cooled conditions with an applied field of 0.5 T. Susceptibility values were corrected for the sample diamagnetism according to Pascal's constants (22) (**AU1-2**, -437×10^{-6}; $(NH_4)_7U_6F_{31}$, -642×10^{-6} emu/f.u.) and for the sample holder diamagnetism.

TABLE 2
Atomic Coordinates and Equivalent Isotropic Displacement Parameters for $(C_5H_{14}N_2)_2U_2F_{12}\cdot 5H_2O$ (AU1-2)

Atom	x	y	z	U_{eq} (Å^2)[a]
U(1)	0.1139(1)	0.2491(1)	0.3166(1)	0.019(1)
U(2)	0.5900(1)	0.1747(1)	0.2191(1)	0.019(1)
F(1)	0.1158(12)	0.1814(4)	0.4067(4)	0.050(2)
F(2)	0.0072(11)	0.3347(3)	0.2515(4)	0.039(2)
F(3)	0.4176(9)	0.3050(3)	0.3655(3)	0.030(2)
F(4)	−0.0371(9)	0.1800(3)	0.2308(3)	0.030(2)
F(5)	−0.2394(9)	0.2397(3)	0.3101(3)	0.029(2)
F(6)	0.0297(11)	0.3152(4)	0.4004(4)	0.044(2)
F(7)	0.3869(9)	0.1669(3)	0.3130(3)	0.027(2)
F(8)	0.3329(9)	0.2618(3)	0.2225(3)	0.027(2)
F(9)	0.6643(12)	0.0786(4)	0.2706(4)	0.045(2)
F(10)	0.6953(11)	0.1139(4)	0.1297(4)	0.045(2)
F(11)	0.3078(10)	0.1395(4)	0.1561(4)	0.039(2)
F(12)	0.6411(10)	0.2539(4)	0.1427(3)	0.034(2)
N(1)	1.0297(17)	0.0309(6)	0.1672(7)	0.050(3)
N(2)	0.8398(16)	−0.1119(5)	0.2103(6)	0.042(3)
N(3)	−0.2684(15)	0.2380(6)	0.4564(5)	0.037(3)
N(4)	−0.4876(15)	0.2330(6)	0.6013(5)	0.038(3)
C(1)	1.1168(24)	0.0211(7)	0.2425(9)	0.058(4)
C(2)	1.1535(25)	−0.0497(8)	0.2674(10)	0.067(5)
C(3)	0.9643(27)	−0.0886(8)	0.2759(7)	0.059(5)
C(4)	0.7635(24)	−0.0586(8)	0.1596(10)	0.059(5)
C(5)	0.9271(31)	−0.0267(8)	0.1258(10)	0.073(5)
C(6)	−0.3117(22)	0.1659(7)	0.4683(7)	0.042(3)
C(7)	−0.2999(24)	0.1440(8)	0.5429(7)	0.051(4)
C(8)	−0.4753(25)	0.1622(8)	0.5805(8)	0.054(4)
C(9)	−0.4862(19)	0.2836(8	0.5433(7)	0.042(4)
C(10)	−0.2851(21)	0.2868(7)	0.5143(7)	0.040(3)
O(1)	0.2158(26)	0.0513(7)	0.4344(11)	0.138(7)
O(2)	0.6666(28)	0.0897(6)	−0.0086(6)	0.112(6)
O(3)	0.3009(23)	0.0332(8)	0.0618(9)	0.119(6)
O(4)	0.5659(21)	0.0106(6)	0.3852(7)	0.086(4)
O(5)	0.8977(40)	−0.0303(14)	0.4524(14)	0.225(11)

[a] U_{eq} is defined as one-third of the trace of the orthogonalized U_{ij} tensor.

Thermal analysis. Thermal data for **AU1-2** and $(NH_4)_7U_6F_{31}$ were collected using a TA Instruments Model 2920 differential scanning calorimeter. Samples (10–20 mg) were encapsulated in aluminum pans and heated at 10°C/min from 25 to 600°C under a nitrogen atmosphere.

RESULTS AND DISCUSSION

Syntheses. The reaction of UO_3 with HF and homopiperazine in aqueous media at 180°C for 72 h results in the formation of $(C_5H_{14}N_2)_2U_2F_{12}\cdot 5H_2O$ (**AU1-2**) and $(NH_4)_7U_6F_{31}$. The former compound also slowly crystallizes from solutions from which $(NH_4)_7U_6F_{31}$ was derived. After crystallization, **AU1-2** does not redissolve in water. We have performed similar reactions at 150, 160, 180, and 200°C and observed that each of these temperature regimes results in the formation of different uranium-containing products (6–9). Our expectation was that the decomposition of homopiperazine to ethylenediamine (6) and ammonium would be driven in part by increased temperature; however, no such correlation could be made. Therefore, we completed the compositional space diagram (23–26) for the UO_3/HF/homopiperazine system and found that template decomposition is instead driven by high ratios of homopiperazine relative to UO_3 and HF, which indicates that homopiperazine is a reducing agent under hydrothermal conditions. Hence, at low homopiperazine concentrations the U(VI) product, $(C_5H_{14}N_2)U_2O_4F_6$, is isolated (8). The oxidation of homopiperazine to diprotonated ethylenediamine and ammonium (and other unincorporated decomposition products) results in the formation of $(C_2H_{10}N_2)U_2F_{10}$ (6) and $(NH_4)_7U_6F_{31}$. Both of these compounds are insoluble in aqueous media and can be prepared independently of homopiperazine; it is important to note that the room temperature reaction of uranium compounds with fluoride in the presence of ammonium typically results in mixtures of $(NH_4)_7U_6F_{31}$ and β-NH_4UF_5 (18, 27).

Structures. The structure of **AU1-2** consists of infinite one-dimensional $^1_\infty[UF_4F_{4/2}]$ chains running down the a axis that are formed from edge-sharing dodecahedral UF_8 units (Fig. 1). The chains create an extensive hydrogen-bonding network with the diprotonated homopiperazinium cations imparting stability to the structure. This network creates two parallel channels measuring 3.7×7.4 Å and 6.5×13 Å that run down the a axis. The occluded water molecules reside in these channels and form a hydrogen-bonding network as shown in Fig. 2. U–F bridging and terminal bond distances range from 2.292(6) to 2.434(6) Å and 2.194(7) to 2.282(7) Å, respectively, and are within normal ranges. The distance between U(1) and U(2) is 4.034(2) Å and is longer than the U–U distances of 3.739(2) and 3.744(1) Å found in $(C_5H_{14}N_2)_2U_2F_{12}\cdot 2H_2O$ (**AU1-1**)

TABLE 3
Atomic Coordinates and Equivalent Isotropic Displacement Parameters for $(NH_4)_7U_6F_{31}$

Atom	x	y	z	U_{eq} (Å^2)[a]
U(1)	0.6101(1)	0.1455(1)	0.4997(1)	0.016(1)
F(1)	0.7540(3)	0.2968(4)	0.5380(5)	0.036(1)
F(2)	0.6110(3)	0.1567(4)	0.7044(6)	0.026(1)
F(3)	0.4502(3)	0.0220(3)	0.5706(5)	0.019(1)
F(4)	0.7148(3)	0.0984(3)	0.5657(5)	0.025(1)
F(5)	0.7110(3)	0.1691(4)	0.3295(5)	0.031(1)
F(6)[b]	0.6960(34)	0.3092(36)	0.3618(28)	0.048(9)
N(1)	0.9150(7)	0.2231(6)	0.5109(9)	0.042(3)
N(2)	$\frac{2}{3}$	$\frac{1}{3}$	$\frac{5}{6}$	0.048(6)

[a] U_{eq} is defined as one-third of the trace of the orthogonalized U_{ij} tensor.
[b] Occupancy of 1/6.

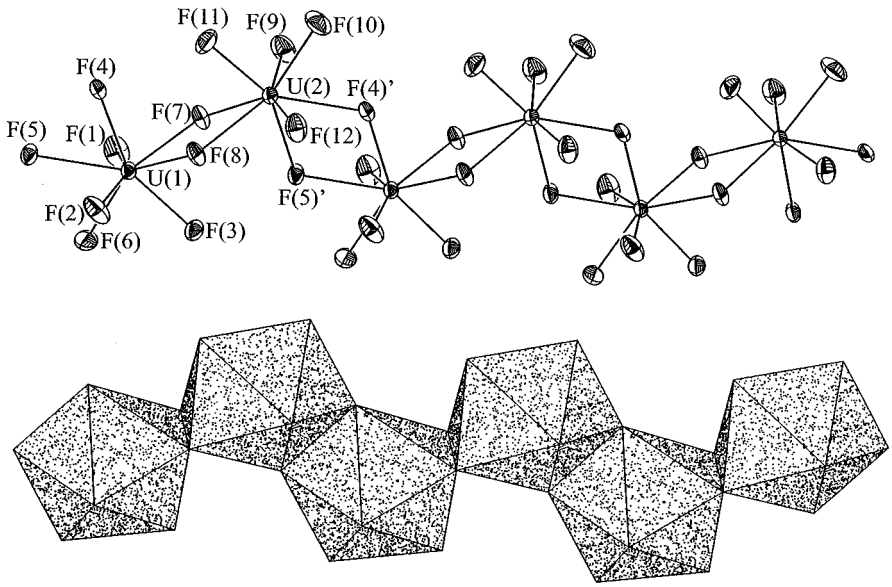

FIG. 1. $[U_2F_{12}]^{4-}$ one-dimensional chains of edge-sharing UF_8 dodecahedra that extend down the *a* axis in **AU1-2**, shown as ball-and-stick (top) and polyhedral representations (bottom). The thermal ellipsoids are drawn at the 50% probability level.

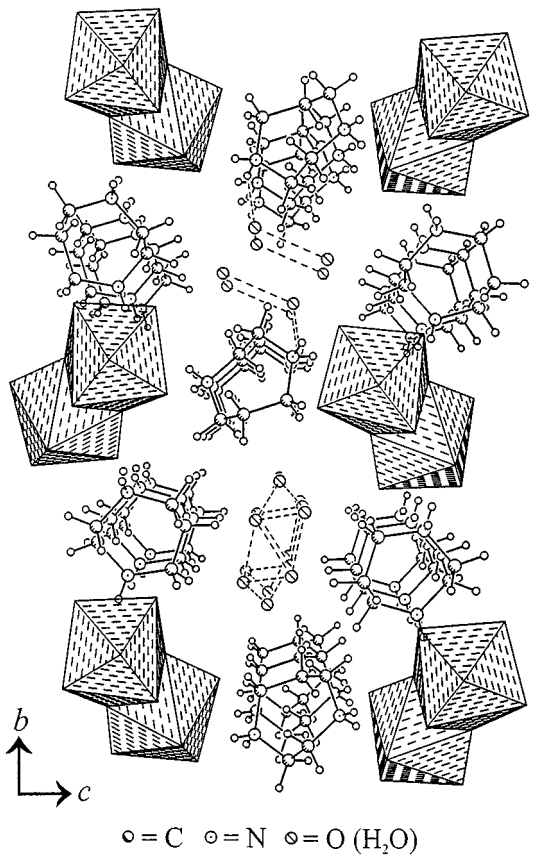

FIG. 2. A view of the hydrogen-bonding network in **AU1-2** showing parallel channels running down the *a* axis and occluded water molecules. The $[U_2F_{12}]^{4-}$ chains are illustrated using polyhedra and most of the hydrogen bonds have been omitted for clarity.

(6). The latter compound contains one-dimensional chains built from face-sharing UF_9 tricapped trigonal prisms (6). Selected bond distances for **AU1-2** are given in Table 4. Similar one-dimensional chains of UF_8 polyhedra have been previously observed in other U(IV) fluorides including α-$(NH_4)_2UF_6$ (28), γ-$(NH_4)_2UF_6$ (29), Rb_2UF_6 (30, 31), and $(C_5H_{14}N_2)_2U_2F_{12} \cdot H_2O$ (3). The geometry about the U(IV) centers varies between square antiprisms, dodecahedra, and bicapped trigonal prisms. Because minor distortions are sufficient to interconvert these CN8 geometries and the observed geometries do not frequently conform to the ideal symmetry, the qualitative description of these coordination polyhedra is inexact at best (29). The bond valence sums for U(1) and U(2) are 4.07 and 4.10, respectively, which are consistent with the structure and formula assignments (32, 33).

$(NH_4)_7U_6F_{31}$ is well known from powder data to be isostructural with $Na_7Zr_6F_{31}$ (17, 29, 34, 35). The structure is composed of UF_8 square antiprisms that edge- and corner-share to form a three-dimensional open-framework network. Each UF_8 unit shares four corners to form a cubooctahedral $(UF_8)_6$ cluster as shown in Fig. 3. A fluoride anion is contained within this cluster. In $Na_7Zr_6F_{31}$, this fluoride anion resides in the center of the cluster. Whereas in $(NH_4)_7U_6F_{31}$, this anion is disordered over six sites and forms long contacts with the surrounding uranium atoms. These differences are most likely a result of the larger size of uranium, which enhances its ability to attain higher coordination numbers. Each UF_8 square antiprism also shares one edge with a neighboring $(UF_8)_6$ cluster.

TABLE 4
Selected Bond Distances (Å) for $(C_5H_{14}N_2)_2U_2F_{12}\cdot 5H_2O$ (AU1-2) and $(NH_4)_7U_6F_{31}$

	$(C_5H_{14}N_2)_2U_2F_{12}\cdot 5H_2O$ (**AU1-2**)		
U(1)–F(1)	2.201(7)	U(2)–F(5)′	2.309(6)
U(1)–F(2)	2.194(7)	U(2)–F(7)	2.396(6)
U(1)–F(3)	2.241(6)	U(2)–F(8)	2.424(6)
U(1)–F(4)	2.292(6)	U(2)–F(9)	2.170(7)
U(1)–F(5)	2.434(6)	U(2)–F(10)	2.282(7)
U(1)–F(6)	2.255(7)	U(2)–F(11)	2.158(7)
U(1)–F(7)	2.336(6)	U(2)–F(12)	2.206(6)
U(1)–F(8)	2.388(6)	U(1)–U(2)	4.034(2)
U(2)–F(4)′	2.419(6)		
	$(NH_4)_7U_6F_{31}$		
U(1)–F(1)	2.307(4)	U(1)–F(6)	2.64(4)
U(1)–F(2)	2.215(6)	U(1)–F(1)′	2.286(5)
U(1)–F(3)	2.359(4)	U(1)–F(3)′	2.383(4)
U(1)–F(4)	2.188(4)	U(1)–F(5)′	2.322(5)
U(1)–F(5)	2.312(5)	U(1)–F(1)′	4.041(1)

Therefore, each cluster is bound to six others. The linking of these clusters into a network creates small intersecting channels that contain the ammonium cations, one view of which is shown in Fig. 4. Selected bond distances are given in Table 4. U–F terminal bond distances are 2.188(4) and 2.215(6) Å. U–F bridging distances range from 2.286(5) to 2.383(4) Å. The shortest U–U distance is 4.041(1) Å and is very close to the U–U distance of 4.034(2) Å found in **AU1-2**. The bond valence sum for U(1) is 4.19, which is consistent with the structure and formula assignment (32, 33).

Magnetic properties. **AU1-2** and $(NH_4)_7U_6F_{31}$ exhibit very similar temperature dependence of the effective moments (Figs. 5a and 5b). The effective moments of μ_{eff} (300 K) = 3.05 and 3.03 μ_B/U(IV) for **AU1-2** and $(NH_4)_7U_6F_{31}$, respectively, fall within the range observed for other organic/inorganic uranium(IV) fluorides (1, 6, 7, 10). The effective moment continues to rise at high temperatures, which is reflected in the large θ values of -97 and -126 K for **AU1-2** and $(NH_4)_7U_6F_{31}$, respectively. This rise is attributed to the presence of thermally populated excited states, although the presence of antiferromagnetic interactions between spin centers may also be contributing

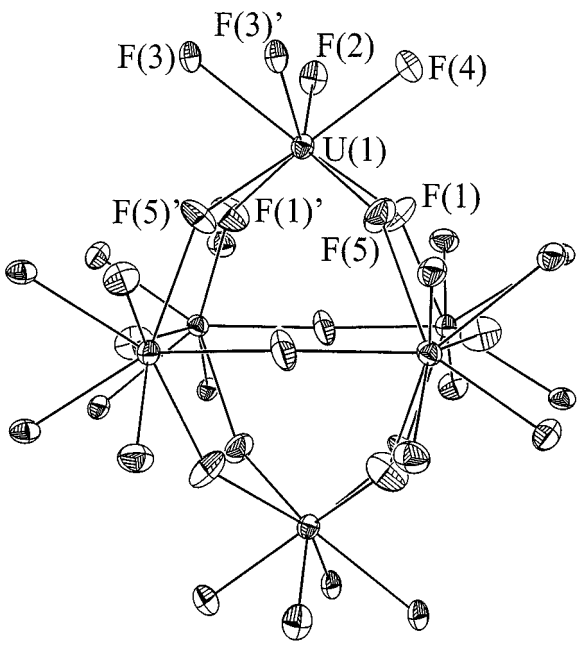

FIG. 3. $(UF_8)_6$ cubooctahedron built from corner-sharing UF_8 square antiprisms in $(NH_4)_7U_6F_{31}$. The thermal ellipsoids are drawn at the 50% probability level. The disordered F(6) atom residing near the center of the cavity has been omitted for clarity.

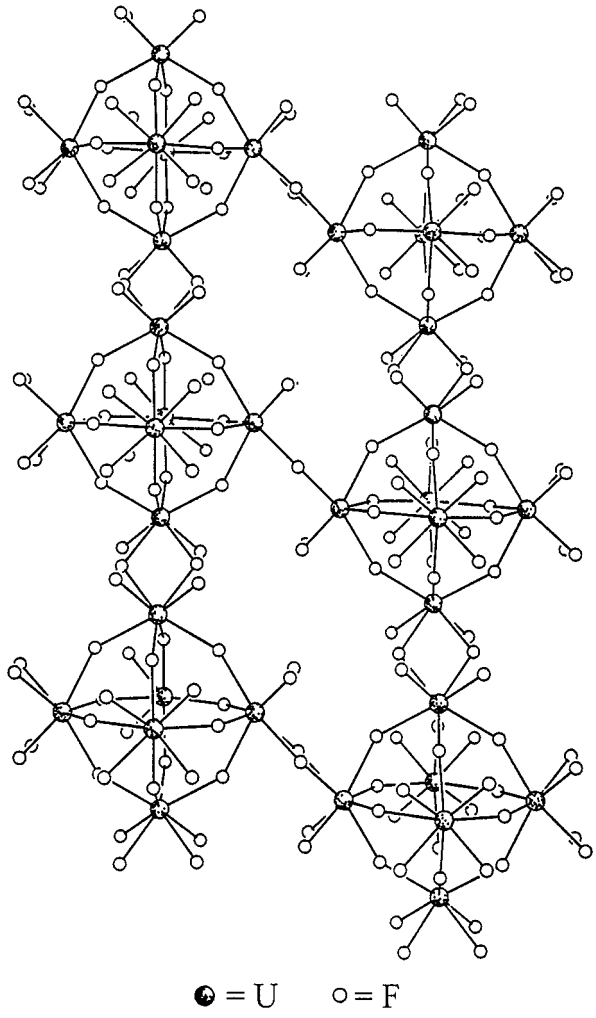

FIG. 4. Network of edge-sharing $(UF_8)_6$ cubooctahedral clusters forming small interconnecting channels in $(NH_4)_7U_6F_{31}$. Nitrogen atoms (from ammonium cations) have been omitted for clarity.

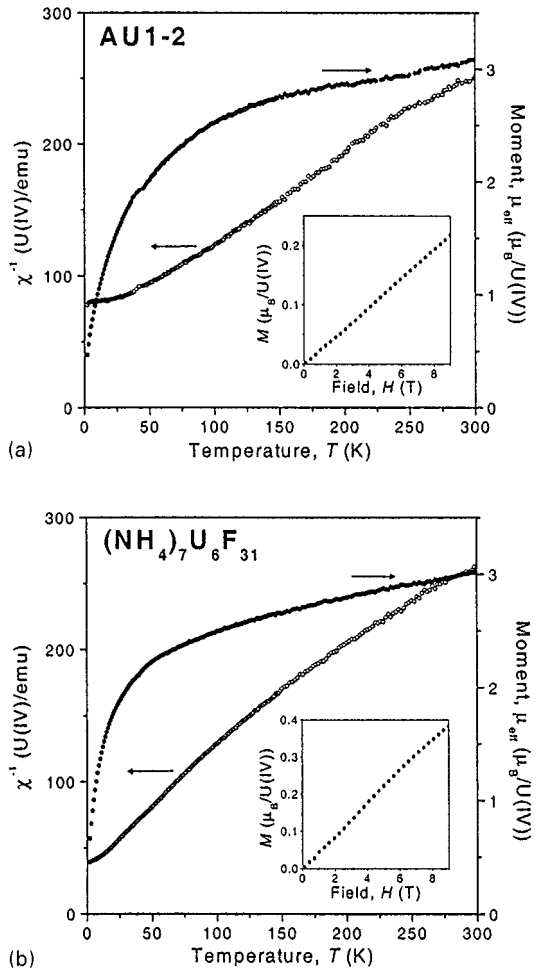

FIG. 5. Effective moment and inverse magnetic susceptibility with $H = 0.5\,\mathrm{T}$ of **AU1-2** (top) and $(NH_4)_7U_6F_{31}$ (bottom). Insets: isothermal magnetization at $T = 2\,\mathrm{K}$.

to the negative θ values. **AU1-2** and $(NH_4)_7U_6F_{31}$ possess very similar U(IV) coordination environments and U–U distances. However, $(C_5H_{14}N_2)_2U_2F_{12}\cdot H_2O$ (**UFO-6**; $\mu_{\mathrm{eff}}(300\,\mathrm{K}) = 3.59\,\mu_B/\mathrm{U(IV)}$) contains a one-dimensional chain with U(IV) coordination and U–U distances similar to those of **AU1-2** and yet shows substantially different magnetic susceptibility behavior (10). The determination of crystalline electric field, spin-orbit, and exchange effects on the temperature dependence of the magnetic susceptibility are then required for a further understanding of the magnetism of these low-dimensional U(IV) fluorides. The isothermal magnetization curves for **AU1-2** and $(NH_4)_7U_6F_{31}$ at $T = 2\,\mathrm{K}$ are essentially linear with fields up to $H = 9\,\mathrm{T}$ with $M_{9\mathrm{T}} = 0.22$ and $0.38\,\mu_B/\mathrm{U(IV)}$, respectively. At very low temperatures, **AU1-2** and $(NH_4)_7U_6F_{31}$ do not show evidence of magnetic ordering. However **AU1-2** displays a leveling off of the magnetic susceptibility below 15 K to 0.013 emu/U(IV), indicative of a nonmagnetic ground state for this compound.

Thermal behavior. The thermal behavior of **AU1-2** and $(NH_4)_7U_6F_{31}$ was evaluated using differential scanning calorimetry from 25 to 600°C. For **AU1-2**, these measurements indicate two well-defined endotherms at 118 and 319°C most likely corresponding to the loss of water and decomposition of the homopiperazinium cations, respectively. These measurements are consistent with thermogravimetric analysis and differential scanning calorimetry measurements for $(C_4H_{12}N_2)ZrF_6\cdot H_2O$ (**AU1-6**), which has a structure similar to that of **AU1-2** (36). In contrast, we have found that two-dimensional uranium and zirconium compounds typically loose water at temperatures closer to 200°C (36). Thermal analysis of $(NH_4)_7U_6F_{31}$ indicates that the onset of decomposition begins at 290°C and peaks at 380°C.

Auxiliary material. Tables of anisotropic displacement parameters and structure factors for **AU1-2** and $(NH_4)_7U_6F_{31}$ (14 pages) are available from the corresponding author upon request.

ACKNOWLEDGMENTS

This work was supported by NASA (Alabama Space Grant Consortium), NASA-EPSCoR, and Auburn University. Financial support from NSERC (Canada) and the University of Alberta is gratefully acknowledged.

REFERENCES

1. R. J. Francis, P. S. Halasyamani, and D. O'Hare, *Chem. Mater.* **10,** 3131 (1998).
2. R. J. Francis, P. S. Halasyamani, and D. O'Hare, *Angew. Chem. Int. Ed. Engl.* **37,** 2214 (1998).
3. R. J. Francis, P. S. Halasyamani, J. S. Bee, and D. O'Hare, *J. Am. Chem. Soc.* **121,** 1609 (1999).
4. P. S. Halasyamani, S. M. Walker, and D. O'Hare, *J. Am. Chem. Soc.* **121,** 7415 (1999).
5. S. M. Walker, P. S. Halasyamani, S. Allen, and D. O'Hare, *J. Am. Chem. Soc.* **121,** 10513 (1999).
6. P. M. Almond, L. Deakin, M. J. Porter, A. Mar, and T. E. Albrecht-Schmitt, *Chem. Mater.* **12,** 3208 (2000).
7. P. M. Almond, L. Deakin, A. Mar, and T. E. Albrecht-Schmitt, *Inorg. Chem.* **40,** 886 (2001).
8. P. M. Almond, C. E. Talley, A. C. Bean, S. M. Peper, and T. E. Albrecht-Schmitt, *J. Solid State Chem.* **154,** 635 (2000).
9. C. E. Talley, A. C. Bean, and T. E. Albrecht-Schmitt, *Inorg. Chem.* **39,** 5174 (2000).
10. S. Allen, S. Barlow, P. S. Halasyamani, J. F. W. Mosselmans, D. O'Hare, S. M. Walker, and R. I. Walton, *Inorg. Chem.* **39,** 3791 (2000).
11. R. J. Francis, M. J. Drewitt, P. S. Halasyamani, C. Ranganathachar, D. O'Hare, W. Clegg, and S. J. Teat, *Chem. Commun.* **2,** 279 (1998).
12. P. S. Halasyamani, R. J. Francis, S. M. Walker, and D. O'Hare, *Inorg. Chem.* **38,** 271 (1999).

13. C. A. Hutchison, Jr., and G. A. Candela, *J. Chem. Phys.* **27,** 707 (1957).
14. (a) J.-M. Fournier and R. Troć *in* "Handbook on the Physics and Chemistry of the Actinides" (A. J. Freeman and G. H. Lander, Eds.), Elsevier, New York, 1985, and references therein. (b) D. H. Martin, "Magnetism in Solids," MIT Press, Cambridge, MA, 1967.
15. T. Yoshimura, C. Miyake, and S. Imoto, *Bull. Chem. Soc. Jpn.* **47,** 515 (1974).
16. M. J. M. Leask, D. W. Osborne, and W. P. Wolf, *J. Chem. Phys.* **34,** 2090 (1961).
17. R. Benz, R. M. Douglass, F. H. Kruse, and R. A. Penneman, *Inorg. Chem.* **2,** 799 (1963).
18. R. A. Penneman, R. R. Ryan, and A. Rosenzweig, *Acta Crystallogr. B* **30,** 1966 (1974).
19. G. M. Sheldrick, SHELXTL PC, Version 5.0, An Integrated System for Solving, Refining, and Displaying Crystal Structures from Diffraction Data. Siemens Analytical X-Ray Instruments, Inc., Madison, WI, 1994.
20. J. F. Mitchell, J. K. Burdett P. M. Keane, J. A. Ibers, D. C. DeGroot, T. P. Hogan, J. L. Schindler, and C. R. Kannewurf, *J. Solid State Chem.* **99,** 103 (1992).
21. Y. V. Mironov, J. A. Cody, T. E. Albrecht-Schmitt, and J. A. Ibers, *J. Am. Chem. Soc.* **119,** 494 (1997).
22. L. N. Mulay and E. A. Boudreaux, "Theory and Applications of Molecular Diamagnetism." Wiley–Interscience, New York, 1976.
23. P. S. Halasyamani, M. J. Willis, P. M. Lundquist, C. L. Stern, G. K. Wong, and K. R. Poeppelmeier, *Inorg. Chem.* **35,** 1367 (1996).
24. W. T. A. Harrison, L. L. Dussack, and A. J. Jacobson, *J. Solid State Chem.* **125,** 234 (1996).
25. A. J. Norquist, K. R. Heier, C. L. Stern, and K. R. Poeppelmeier, *Inorg. Chem.* **37,** 6495 (1998).
26. A. J. Norquist, M. E. Welk, C. L. Stern, and K. R. Poeppelmeier, *Inorg. Chem.* **12,** 1905 (2000).
27. Allied Chemical Corporation (1970). British Patent No. 1 183 268, March 4, 1970.
28. R. A. Penneman, F. H. Kruse, R. S. George, and J. S. Coleman, *Inorg. Chem.* **3,** 309 (1964).
29. R. A. Penneman, R. R. Ryan, and A. Rosenzweig, *Struct. Bonding* **13,** 1 (1973).
30. F. H. Kruse, *J. Inorg. Nucl. Chem.* **33,** 1625 (1971).
31. T. K. Keenan, *Inorg. Nucl. Chem. Lett.* **3,** 463 (1967).
32. I. D. Brown, D. Altermatt, *Acta Crystallogr. B* **41,** 244 (1985).
33. N. E. Brese, M. O'Keeffe, *Acta Crystallogr. B* **47,** 192 (1991).
34. R. E. Thoma, *Inorg. Chem.* **1,** 220 (1962).
35. J. H. Burns, R. D. Ellison, and H. A. Levy, *Acta Crystallogr. B* **24,** 230 (1968).
36. R. E. Sykora, M. Ruf, and T. E. Albrecht-Schmitt, *J. Solid State Chem.*, in press.